Thermal decomposition of struvite –implications for the decomposition of kidney stones

Ray L. Frost•, Matt L. Weier and Kristy L. Erickson

Inorganic Materials Research Program, School of Physical and Chemical Sciences, Queensland University of Technology, GPO Box 2434, Brisbane, Queensland 4001, Australia.

Published as:
R.L. Frost, M.L. Weier, and K.L. Erickson, Thermal decomposition of struvite. Journal of Thermal Analysis and Calorimetry, 2004. 76(3): p. 1025-1033

Abstract

Struvite ($NH_4MgPO_4.6H_2O$) is a mineral often found in urinary tracts and kidneys. Thermal decomposition using slow low heating shows that the 'kidney' stone can be decomposed at temperatures below 40 °C. At this temperature both ammonia and water are evolved. If more rapid heating is employed the decomposition occurs at around 80 °C. The implication of this work rests with the use of low slow heat for the decomposition of the kidney stones.

Keywords: strunzite, phosphate, high resolution thermogravimetric analysis, hot stage Raman spectroscopy, infrared emission spectroscopy

Introduction

Large crystals from archaeological deposits in Amsterdam, Holland, proved to be the mineral struvite [1]. The mineral was formed from human waste in old latrines. The mineral goes by other names including guanite. Interest in struvite formation also comes from the formation in urinary tracts and kidneys [2-7]. Indeed the discovery of newberyite have been found in very old and large calculi [8]. The mineral has been found on ivory and is formed through the chemical treatment of ivory [9]. More often than not the presence of struvite has been determined by infrared spectroscopy [10-18]. On occasions Raman spectroscopy has also been used to study the presence of struvite in urine [11, 19, 20]. The mineral struvite has the formula ($NH_4MgPO_4.6H_2O$) and is orthorhombic [21]. The mineral is related to dittmarite ($NH_4MgPO_4.H_2O$), niahite ($NH_4(Mn,Mg)PO_4.6H_2O$), hannayite ($(NH_4)_2MgH_4(PO_4)_4.6H_2O$), schertelite ($(NH_4)_2MgH_2(PO_4)_4.4H_2O$), stercorite ($Na(NH_4)_2HPO_4.4H_2O$), swaknoite ($Ca(NH_4)_2(HPO_4)_2.H_2O$), and mundrabillaite ($(NH_4)_2CaHPO4.H_2O$). Many of these minerals are found in caves and are the result of formation from guano [22-26].

The thermal decomposition of struvite has been studied many times, no doubt because of its occurrence in urinary tracts [27, 28]. The thermal decomposition and infrared spectrum of struvite has been published [29]. The decomposition of struvite

• Author for correspondence (r.frost@qut.edu.au)

has found to be dependent upon the conditions of decomposition. The decomposition is different in nitrogen or in a moist atmosphere. The decomposition is dependent upon the partial pressure of water [27, 28]. In studies of the thermal decomposition of struvite it was found that firstly five moles of water were lost, and then 1 mole of water and finally 1 mole of water together with 0.5 moles of water. It was found that the sequence of the four Q-TG curves became irregular when different sample holders were used. This allowed the following conclusions to be made. If a process involves more than one overlapping reaction, each reaction having different transformation temperatures, then each reaction will collectively contribute the course of the resultant curve. Recently thermoanalytical techniques have been used to study some quite complex mineral and surface modified mineral systems [30-32]. Although thermal analysis has been used for the study of minerals related to struvite, no thermoanalytical studies have been undertaken [33]. In this work we report some thermal analysis studies of struvite and study the structural changes of struvite through thermal decomposition.

EXPERIMENTAL

Thermal analysis

Thermal decomposition of struvite was carried out in a TA® Instruments incorporated high-resolution thermogravimetric analyzer (series Q500) in a flowing nitrogen atmosphere (80 cm^3/min). Approximately 50mg of sample was heated in an open platinum crucible at a rate of 1.0 °C/min up to 500°C. The TGA instrument was coupled to a Balzers (Pfeiffer) mass spectrometer for gas analysis. Only selected gases were analyzed.

Raman microprobe spectroscopy

Samples of struvite from the Museum Victoria collection were placed and orientated on the stage of an Olympus BHSM microscope, equipped with 10x and 50x objective lenses, as part of a Renishaw 1000 Raman microscope system. This system also includes a monochromator, filter system and a Charge Coupled Device (CCD). Raman spectra were excited by a HeNe laser (633 nm) at a resolution of 2 cm^{-1} in the range between 100 and 4000 cm^{-1}. Repeated acquisition using the highest magnification was accumulated to improve the signal to noise ratio. Spectra were calibrated using the 520.5 cm^{-1} line of a silicon wafer. In order to ensure that the correct spectra were obtained, the incident excitation radiation was scrambled, while spectra at controlled temperatures were obtained using a Linkam thermal stage (Scientific Instruments Ltd, Waterfield, Surrey, England).

Infrared absorption spectroscopy

Infrared spectra were obtained using a Nicolet Nexus 870 FTIR spectrometer with a smart endurance single bounce diamond ATR cell. Spectra over the 4000–525 cm^{-1} range were obtained by the co-addition of 64 scans with a resolution of 4 cm^{-1} and a mirror velocity of 0.6329 cm/s. The Spectracalc software package GRAMS was used for data analysis. Band component analysis was undertaken using the Jandel

'Peakfit' software package, which enabled the type of fitting function to be selected and allows specific parameters to be fixed or varied accordingly. Band fitting was carried out using a Gauss-Lorentz cross-product function with the minimum number of component bands used for the fitting process. The Gauss-Lorentz ratio was maintained at values greater than 0.7 and fitting was undertaken until reproducible results were obtained with squared regression coefficient of R^2 greater than 0.995.

RESULTS AND DISCUSSION

Thermal analysis

The theoretical mass loss for the formula ($NH_4MgPO_4.6H_2O$) is 51.42 %. This is made up of mass loss of water as 44.08 % and ammonia as 7.34 (6) %. Figure 1 displays the temperature with time graph. The graph shows the rate of heating is very slow for the initial stages of the experiment. Figure 2 displays the TG of struvite. Figure 3 shows the evolved gas mass gain for the thermal decomposition of struvite. This figure shows that by using a heating rate of 2 degrees per minute and resolution 4 the ammonia and water are lost simultaneously. The temperature of the thermal decomposition is 85 °C. By slowing the thermal decomposition by using 1 °C per minute and resolution 8, the thermal analysis patterns as shown in Figure 4 is obtained. Now three mass loss steps at 39.5, 57.8 and 82.6 °C are obtained. The total mass loss in the HRTG experiment is 42 %. If the assumption is made that all the ammonia is lost as NH_3, then the mass loss of water is 34.65 %. This makes a total of 4.7 moles of water which is 1.3 moles than predicted from the theoretical formula. The struvite being a sample from an archaeological site may contain additional adsorbed water. The low temperature mass loss at 39.5 °C is of significance as it means that low temperature heating causes the decomposition of the struvite. The results for the thermal decomposition of this sample differ from previously published data. In this work the decomposition has been found to be dependent upon the rate of heating. The thermal decomposition at very low heating rates shows that the ammonia is lost before the water of crystallisation. Previous studies have shown the loss of five moles of water followed by 1 mole followed by 1 mole of ammonia [27, 29].

Spectroscopy of the thermally treated struvite

The infrared spectrum of struvite shows four bands at 3693, 3584, 3472 and 3170 cm^{-1} (Figure 5). The transmittance spectrum of struvite has been published [29]. The two most intense bands are observed at 2968 and 2508 cm^{-1}. The analyses of the infrared and Raman spectra of the unheated struvite and the thermally treated struvite are reported in Table 1. The first four bands are attributed to OH stretching vibrations whilst the latter two bands are assigned to the antisymmetric and symmetric stretching vibrations of the NH_4 units. Upon thermal treatment of the struvite, a broad band is observed at 3267 cm^{-1} and is attributed to OH stretching bands of adsorbed water. The position of this band suggests that the water is strongly hydrogen bonded to the Mg cations. The Raman spectrum of struvite shows bands at 3239, 3115 and 2921 cm^{-1} with additional bands at 2903 and 2368 cm^{-1}. Upon thermal treatment these bands are lost. After thermal treatment a

broad low intensity band at 3650 cm^{-1} is observed. This band is assigned to adsorbed water.

The infrared spectrum of struvite displays a set of bands at 1675, 1591 and 1440 cm^{-1}. The first band is assigned to the HOH deformation of water, the next two bands to the HNH deformation modes of NH_4 units. These bands are absent in the thermally treated struvite, although low intensity bands are observed at 1658 and 1596 cm^{-1}. These bands are attributed to water bending modes. Raman spectra show no bands in this region. The infrared spectra of the unheated struvite show two bands at 980 and 1065 cm^{-1}. These bands are assigned to the ν_3 antisymmetric stretching vibrations. The equivalent bands are the bands at 1077 and 1013 cm^{-1} in the Raman spectra. The band at 949 cm^{-1} not observed in the infrared spectrum is ascribed to the ν_1 symmetric stretching vibration. After thermal treatment, PO_4 antisymmetric stretching modes are observed at 997, 1059 and 1125 cm^{-1} in the infrared spectrum and at 970, 1077 and 1247 cm^{-1} in the Raman spectrum. This spectrum closely matches the spectrum of magnesium pyrophosphate and confirms the results of the X-ray diffraction of the thermally decomposed struvite.

The infrared bands at 678 and 748 cm^{-1} are ascribed to the water librational and NH_4 rocking modes. These bands are not observed after thermal treatment. Two bands are observed in the infrared spectrum at 567 and 552 cm^{-1} and are assigned to the ν_4 bending modes of the PO_4 units. After thermal treatment, these bands are observed at 597 and 560 cm^{-1}. In the Raman spectrum a band is observed at 564 cm^{-1} and is assigned to this vibration. Two bands are observed at 463 and 428 cm-1 and are attributed to the ν_2 bending modes. These bands are not observed in the thermally treated struvite. Other bands are observed at 300, 242, 228 and 206 cm^{-1} and are simply described as lattice vibrations.

Conclusions

Struvite is a mineral which is often found in urine and is known as ‘urine sand, in urinary tracts and in kidneys as kidney stones. This experiment has shown that the mineral can be decomposed by prolonged thermal treatment at quite low temperatures. This means that relief from the pain of kidney stones may be induced through warm heating of the kidney region. This experiment has shown the struvite can be decomposed at temperatures below 40 °C. The thermal decomposition of struvite was found to be dependent upon the heating rate.

Acknowledgments

The financial and infra-structure support of the Queensland University of Technology Inorganic Materials Research Program is gratefully acknowledged. The Australian Research Council (ARC) is thanked for funding. Professor R. Schuiling is thanked for the struvite sample from the Amsterdam archaeological site.

References

1. J. M. A. R. Wevers, H. Kars and R. D. Schuiling, Bulletin de Mineralogie 104 (1981) 686.
2. H. J. Schneider and M. Anke, UROLOGIA INTERNATIONALIS FIELD Publication Date:1969 24 300.
3. H. J. Schneider, L. Klotz and G. Horn, ZEITSCHRIFT FUR UROLOGIE UND NEPHROLOGIE FIELD Publication Date:1969 62 351.
4. H. J. Schneider, ZEITSCHRIFT FUR UROLOGIE UND NEPHROLOGIE FIELD Publication Date:1969 Feb 62 123.
5. H. J. Schneider and G. Horn, ZEITSCHRIFT FUR UROLOGIE UND NEPHROLOGIE FIELD Publication Date:1968 Nov 61 753.
6. H. J. Schneider and M. Anke, ZEITSCHRIFT FUR UROLOGIE UND NEPHROLOGIE FIELD Publication Date:1968 Jun 61 361.
7. H. J. Schneider and M. Anke, Zeitschrift fuer Urologie und Nephrologie 61 (1968) 361.
8. K. Lonsdale and D. J. Sutor, Science (Washington, DC, United States) 154 (1966) 1353.
9. A. Freund, G. Eggert, H. Kutzke and B. Barbier, Studies in Conservation 47 (2002) 155.
10. M. Daudon, C. Marfisi, B. Lacour and C. Bader, Clinical Chemistry (Washington, DC, United States) 37 (1991) 83.
11. M. Daudon, M. F. Protat, R. J. Reveillaud and H. Jaeschke-Boyer, Kidney International 23 (1983) 842.
12. E. Escolar and J. Bellanato, Biospectroscopy 5 (1999) 237.
13. M. H. Gault, M. Ahmed, J. Kalra, I. Senciall, J. Morgan, W. Cohen and D. Churchill, Urolithiasis: Clincial Basic Res., [Proc. Int. Symp.], 4th (1981) 993.
14. A. Hesse, M. Gergeleit, P. Schueller and K. Moeller, Journal of Clinical Chemistry and Clinical Biochemistry 27 (1989) 639.
15. A. Khaliq, J. Ahmed and N. Khalid, British Journal of Urology 56 (1984) 135.
16. W. E. Klee, Fortschritte der Urologie und Nephrologie 9 (1977) 234.
17. Y. G. Kozlovsky, M. M. Shokarev and F. I. Vershinina, Laboratornoe Delo (1977) 659.
18. C. Paluszkiewicz, M. Galka, W. Kwiatek, A. Parczewski and S. Walas, Biospectroscopy 3 (1997) 403.
19. K. Sudlow and A. Woolf, Clinica Chimica Acta 203 (1991) 387.
20. K. Angoni, J. Popp and W. Kiefer, Spectroscopy Letters 31 (1998) 1771.
21. J. A. Bland and S. J. Basinski, Nature (London, United Kingdom) 183 (1959) 1385.
22. P. J. Bridge, Mineralogical Magazine 39 (1973) 467.
23. P. J. Bridge, Mineralogical Magazine 41 (1977) 33.
24. P. J. Bridge and R. M. Clark, Mineralogical Magazine 47 (1983) 80.
25. P. J. Bridge and B. W. Robinson, Mineralogical Magazine 47 (1983) 79.
26. R. J. Bowell, A. Warren and I. Redmond, Geological Society Special Publication 113 (1996) 63.
27. G. Liptay and Editor, *Atlas of Thermoanalytical Curves. (TG [Thermogravimetric], DTG [Differential Thermogravimetric], and DTA [Differential Thermoanalytical] Curves Measured Simultaneously), Vol. 4*, 1975.
28. G. Liptay, Revistade Chimie (Bucharest, Romania) 26 (1975) 149.
29. H. J. Schneider, Thieme, Leipzig (1974).

30. R. L. Frost, Z. Ding and H. D. Ruan, Journal of Thermal Analysis and Calorimetry 71 (2003) 783.
31. E. Horvath, R. L. Frost, E. Mako, J. Kristof and T. Cseh, Thermochimica Acta 404 (2003) 227.
32. E. Horvath, J. Kristof, R. L. Frost, A. Redey, V. Vagvolgyi and T. Cseh, Journal of Thermal Analysis and Calorimetry 71 (2003) 707.
33. M. Franchini-Angela, Atti della Accademia delle Scienze di Torino, Classe di Scienze Fisiche, Matematiche e Naturali (1974) 757.

Raman				IR			
Struvite		Heat Treated		Struvite		Heat Treated	
Center	Area	Center	Area	Center	Area	Center	Area
				3693	0.000	3695	0.002
		3650	0.004				
				3584	0.002		
				3472	0.010		
						3416	0.080
3239	0.023						
				3170	0.069		
						3139	0.256
3115	0.181						
2921	0.083						
2903	0.001	2903	0.002				
				2868	0.530		
						2792	0.033
				2508	0.073		
2368	0.041						
				2332	0.059		
				1803	0.010		
				1675	0.005	1658	0.007
				1591	0.043	1596	0.018
				1440	0.006		
		1247	0.017				
						1125	0.088
1077	0.017	1077	0.428	1065	0.003	1059	0.152
1013	0.014						
		970	0.471	980	0.074	997	0.124
949	0.042					949	0.010
942	0.352						
890	0.015			894	0.055	883	0.060
				748	0.019		
				678	0.005		
		614	0.046			630	0.006
						597	0.005
564	0.094	572	0.032	567	0.003	560	0.014
				552	0.004		
463	0.011						
428	0.016						
300	0.060						
242	0.016						
228	0.015						
206	0.024	206	0.060				

Table 1 Results of the Raman and infrared spectra of the unheated and thermally decomposed struvite.

List of Figures

List of Tables

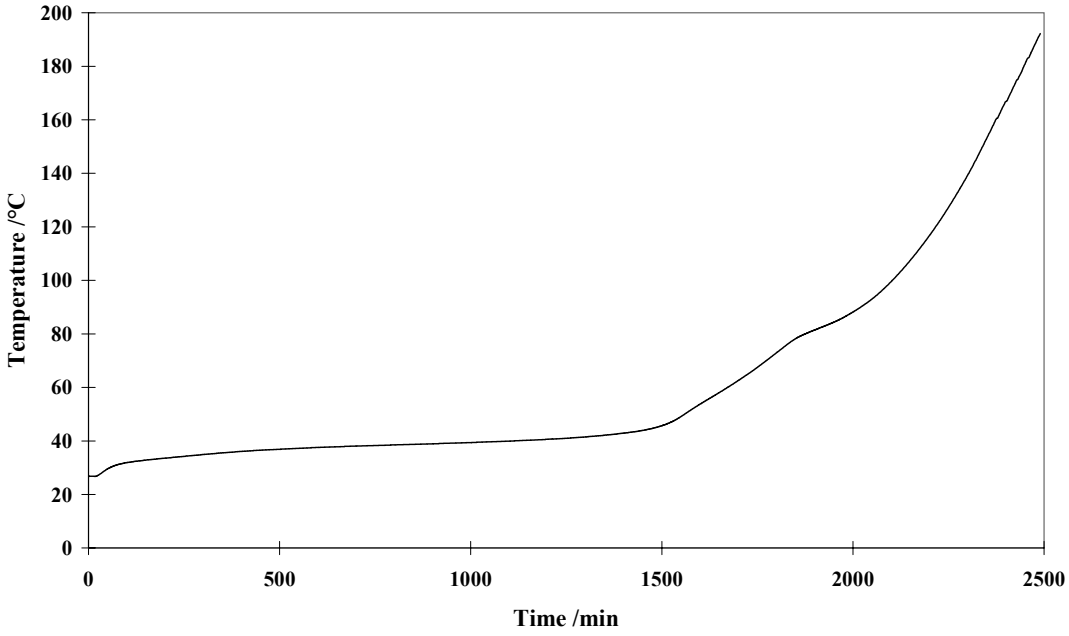
Temperature /°C
200
180
160
140
120
100
80
60
40
20
0
0
500
1000
1500
2000
2500
Time /min

Figure 1

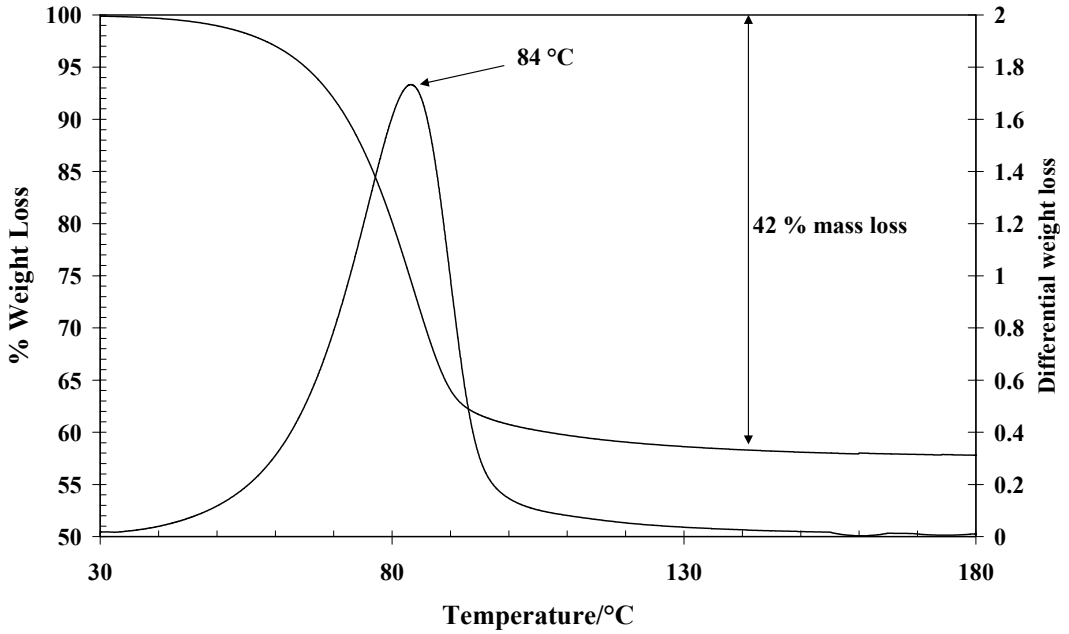

Figure 2

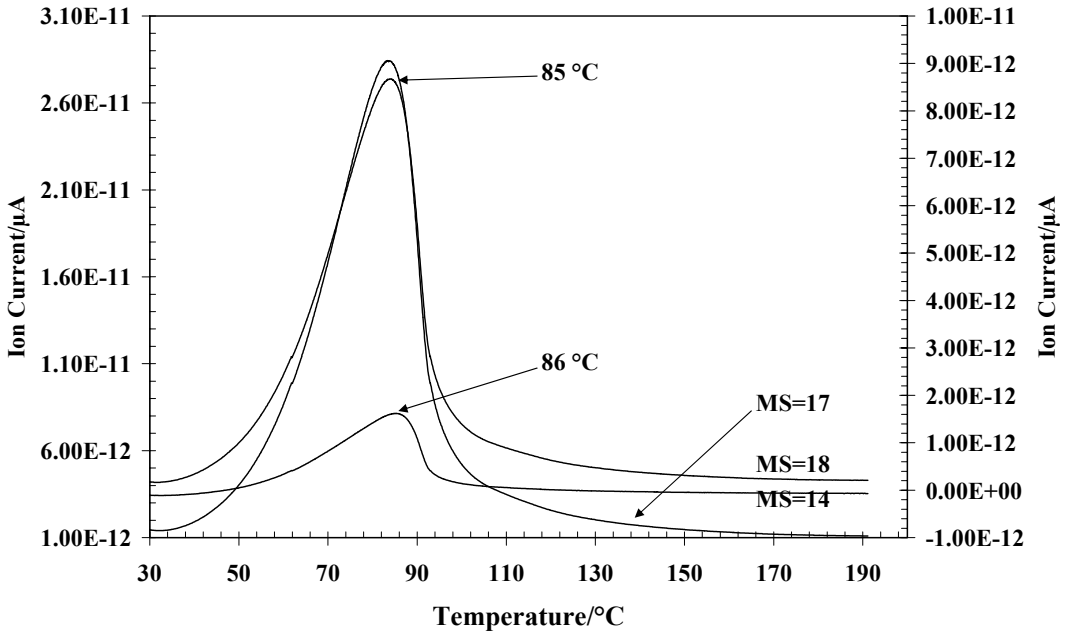

Figure 3

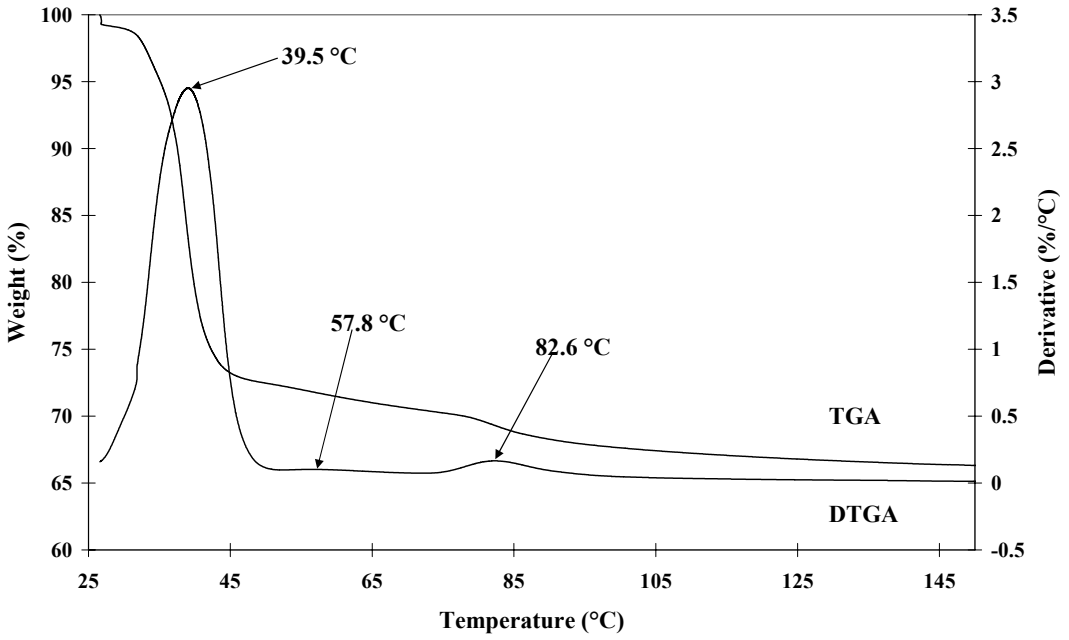
100
95
90
85
80
75
70
65
60
Weight (%)
3.5
3
2.5
2
1.5
1
0.5
0
-0.5
Derivative (%/°C)
39.5 °C
57.8 °C
82.6 °C
TGA
DTGA
25
45
65
85
105
125
145
Temperature (°C)

Figure 4

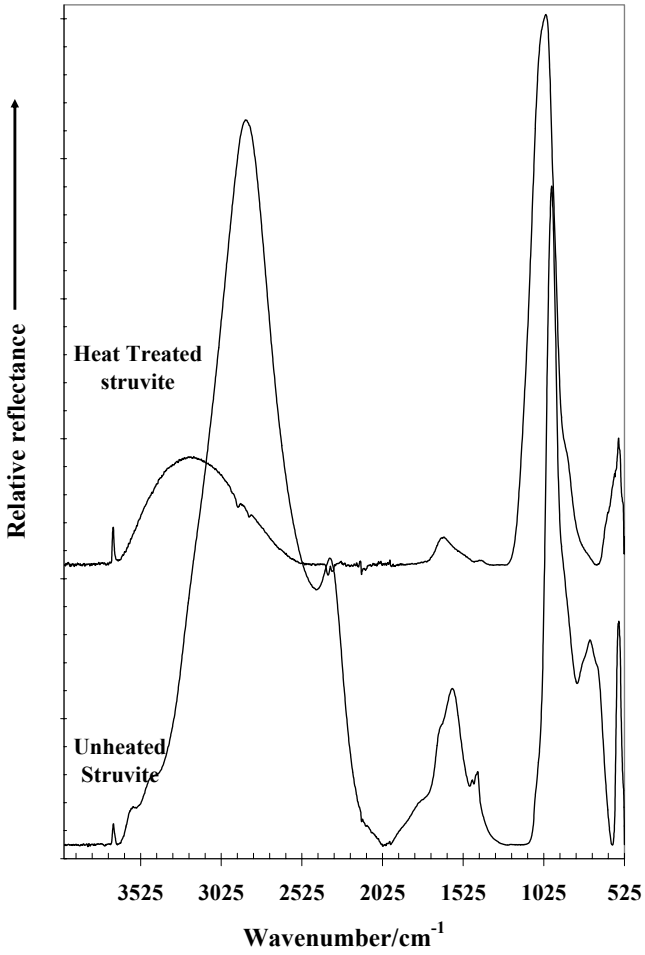
Relative reflectance
Heat Treated
struvite
Unheated
Struvite
3525
3025
2525
2025
1525
1025
525
Wavenumber/cm-1

Figure 5

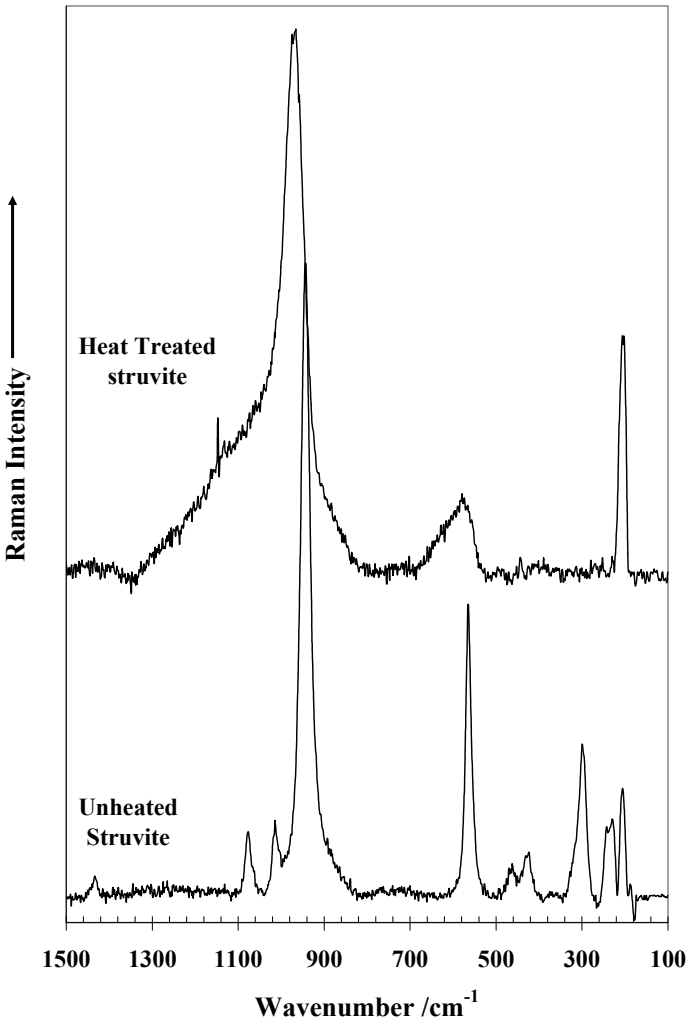
Raman Intensity
Heat Treated
struvite
Unheated
Struvite
1500
1300
1100
900
700
500
300
100
Wavenumber /cm-1

Figure 6